Separated Flow Unsteady Aerodynamic Theory

R. M. Chi*
United Technologies Research Center, East Hartford, Connecticut

A relatively simple two-dimensional subsonic unsteady aerodynamic theory has been developed to take into account approximately the effect of flow separation on unsteady airloads for high incidence angles of thin airfoil sections. The theory is an extension of the classical linear potential flow theory for thin airfoils with proper boundary conditions applied to the flow separation region along the airfoil surface. The mixed boundary value problem for the lifting unsteady aerodynamics is translated into two singular integral equations that are solved by using the collocation method. Very encouraging correlation has been obtained between the calculated and experimental pitch damping values for a thin airfoil section typical of propeller blade at large angles of attack.

Nomenclature

a_∞ = undisturbed upstream sound speed
A = nonlifting kernel function
c = blade full chord
$C(x,\xi)$ = see Eq. (29)
C_L = section lift coefficient
C_M = section moment coefficient
D/Dt $\equiv (\partial/\partial t) + U(\partial/\partial_x)$
f = amplitude of harmonic $\hat{f}$
$\hat{f}$ = airfoil normal displacement
h = amplitude of harmonic heaving motion
$H_n^{(2)}$ = Hankel function of the second kind of nth order
Im{ } = imaginary part of { }
J_ν = Bessel function of the first kind of order ν
$K(x-\xi)$ = lifting kernel function
$\ell(x)$ = see Eq. (28)
M = Mach number
p = amplitude of harmonic $\hat{p}$
$\hat{p}$ = perturbation pressure
Δp $\equiv p_+ - p_-$
P_0 = eigensolution for $\Delta p/\rho U^2$
P_1 = unit upwash solution for $\Delta p/\rho U^2$ satisfying leading-edge Kutta condition
$\hat{P}_1$ = unit upwash solution for $\Delta p/\rho U^2$ satisfying trailing-edge Kutta condition
Re{ } = real part of { }
sgn = sign function
t = time
U or U_∞ = undisturbed upstream flow velocity
W = upwash velocity
$\bar{W}$ $\equiv \frac{1}{2}(W_+ + W_-)$
ΔW $\equiv W_+ - W_-$
Y_ν = Bessel function of the second kind of order ν
x = coordinate in direction of undisturbed upstream flow velocity
x_0 = axis about which the moment is taken
x_{PCH} = pitching axis x coordinate
x_s = flow separation point x coordinate
z = coordinate vertical to x
α = Fourier transform variable
β $= \sqrt{1-M^2}$
γ = cavitation function
$\Gamma()$ = Gramma function
Γ_K = inversion kernel corresponding to K
θ = amplitude of harmonic pitching motion
ξ^* $= (\xi - x_s)/(1-x_s)$
π = 3.14159...
ρ = fluid density
ϕ = perturbation velocity potential
ω = circular frequency
∇^2 = Laplacian operator

Superscript

( )* = Fourier transform

Subscripts

NS = nonseparated flow
COR = correction due to flow separation
+ = upper blade surface
− = lower blade surface
α = pitching motion
h = plunging motion

Presented as Paper 84-0874 at the AIAA/ASME/ASCE/AHS 25th Structures, Structural Dynamics and Materials Conference, Palm Springs, CA, May 14-17, 1984; received June 4, 1984; revision received July 23, 1985.

*Senior Research Engineer. Member AIAA.

I. Introduction

FOR the major reason of high fuel efficiency, the development of advanced propfans has been of renewed interest to the general aviation industry.[1] The propeller diameter of typical advanced turboprop propulsion systems is kept small by the use of many blades. These propeller blades are ultrathin and highly swept in order to maintain high efficiency in the tip region. As a result of the high-performance aerodynamic design, a stall flutter problem has been experienced in recent wind tunnel tests.[2] Therefore, the avoidance of stall flutter of the new generation propfan blades has become a major concern in blade structural design.

The major deficiency in the current flutter design system is the lack of a practical unsteady aerodynamic theory applicable to stalled compressible flow surrounding ultrathin blades. The aerodynamics of high angles of attack for stalled flows involving flow separation is a classical research subject. A concise discussion on the steady-flow separation characteristics at low and transonic speeds was given by Smith.[3] For unsteady separated flows, Ericsson and Reding[4-7] have developed semiempirical analysis procedures for dynamic stall airloads based on static airfoil stall performance characteristics. More exact treatments of unsteady separated flows by carefully modeling the bound and free vortex sheets are given by Ham[8] and Kandil and colleagues.[9-11]

In this paper, a theoretical unsteady aerodynamic model is described to account for the effect of flow separations on stalled unsteady airloads in the subsonic flow regime. The flow model modifies the classical potential flow model by specifying the separation point position and unsteady pressure in the separated region. Flow models of a similar type have been used in the past by Woods[12] in his study of airfoils with spoilers in an incompressible flow, Wu[13] in his wake and cavity flow theory development, Perumal and Sisto[14] in their study of incompressible unsteady flow with a moving flow separation point, Dowell[15] in his transonic unsteady aerodynamic study for isolated airfoils, and Chi[16] in his subsonic stall flutter study of cascade blades. The present work deals with a subsonic flow about an isolated thin airfoil with a fixed flow separation point, which is taken as the leading edge for all calculations. The assumption of leading-edge flow separation is certainly a serious limitation and is probably applicable only to small-amplitude vibrations of airfoils with a sharp leading edge, such as the NACA 16-series airfoils shown below in Fig. 6. The theory provides a new derivation of the classical lifting and nonlifting kernel functions (aerodynamic influence functions or Green's functions). It utilizes both the classical lifting and nonlifting kernel functions in the analysis of separated flow lifting aerodynamics. Sample calculation results based on the present theory are compared with other theories and, more importantly, with aerodynamic damping test data for typical thin NACA airfoils used in propfan designs.

In the following discussion, the theory will be presented first, followed by a discussion on the correlation between the calculated force coefficients with other theoretical and experimental data. Conclusions will then be drawn and recommendations on future work to further advance the stalled airload technology will be made.

II. Theory

Governing Equations

The perturbation velocity potential $\hat{\phi}$ is assumed to satisfy the convective wave equation

$$\nabla^2\hat{\phi}=\frac{1}{a_\infty^2}\frac{\mathrm{D}^2\hat{\phi}}{\mathrm{D}t^2} \tag{1}$$

where a_∞ is the undisturbed upstream sound speed and

$$\frac{\mathrm{D}}{\mathrm{D}t}\equiv\frac{\partial}{\partial t}+U_\infty\frac{\partial}{\partial x}$$

The perturbation pressure $\hat{p}$ is related to the perturbation velocity potential $\hat{\phi}$ by Bernoulli's equation

$$\hat{p}=-\rho_\infty\left(\frac{\partial\hat{\phi}}{\partial t}+U_\infty\frac{\partial\hat{\phi}}{\partial x}\right) \tag{2}$$

where ρ_∞ is the undisturbed upstream density and U_∞ the undisturbed upstream velocity.

The coordinate x is chosen to be in the freestream direction, z is perpendicular to x, and t denotes time. The origin of the x,z coordinate system is fixed at the leading edge of the airfoil as shown in Fig. 1 and all linear dimensions are scaled by the blade chord c.

For simple harmonic motion, we have

$$\hat{\phi}=\phi e^{i\omega t}$$

$$\hat{p}=pe^{i\omega t}$$

$$\beta^2\frac{\partial^2\phi}{\partial x^2}+\frac{\partial^2\phi}{\partial z^2}-2i\frac{\omega}{U}M^2\frac{\partial\phi}{\partial x}+\left(\frac{\omega}{U}M\right)^2\phi=0 \tag{3}$$

$$\frac{p}{\rho U}=-\left(i\frac{\omega}{U}+\frac{\partial}{\partial x}\right)\phi \tag{4}$$

where $\beta=\sqrt{1-M^2}$ and M is the upstream Mach number. For convenience, the subscript ∞ has been dropped for all upstream flow quantities.

Boundary Conditions

When there is no flow separation, the following boundary conditions apply:

1) On the airfoil surface, the flow tangency condition is assumed, i.e.,

$$\phi_z=\hat{W} \tag{5}$$

where $\hat{W}$ is the prescribed upwash velocity. This boundary condition applies to both the upper and lower surfaces of the airfoil.

2) Off the airfoil, the perturbation pressure and vertical velocity (upwash) are continuous everywhere.

3) The radiation/finiteness condition is satisfied at infinity.

For simple harmonic motion, the blade displacement is simply

$$\hat{f}(x,t)=f(x)e^{i\omega t}$$

Since the upwash is related to the blade displacement by

$$\hat{W}=\frac{\partial\hat{f}}{\partial t}+U\frac{\partial\hat{f}}{\partial x}$$

or, for simple harmonic motion,

$$\hat{W}=We^{i\omega t}$$

$$W=\left(i\omega+U\frac{\partial}{\partial x}\right)f$$

the upwash $W(x)$ is given for $x\epsilon(0, 1)$ and unknown otherwise. For combined pitching and heaving motion in nonseparated (attached) flow,

$$W(x)=i\omega h-[i\omega(x-x_{\mathrm{PCH}})+U]\theta$$

$$=(i\omega h-U\theta)-i\omega(x-x_{\mathrm{PCH}})\theta$$

where x_{PCH} is the pitching axis location and h and θ are the heaving and pitching amplitude, respectively. Therefore, the boundary condition is

$$\phi_z=W(x)=(i\omega h-U\theta)-i\omega(x-x_{\mathrm{PCH}})\theta \tag{6}$$

For attached flows, the boundary conditions described above are adequate. For separated flow, we modify the boundary condition on the airfoil surface [Eq. (5)] by assuming that the perturbation pressure $\hat{p}$ is known in the flow separation region and defining the cavitation function γ as

$$\gamma=\frac{p_\infty-p_+}{\frac{1}{2}\rho U^2}=\frac{-\hat{p}_+}{\frac{1}{2}\rho U^2} \tag{7}$$

The same asumption was made previously by Perumal and Sisto,[14] Dowell,[15] and Chi,[16] among others, except that they assumed a zero cavitation. The assumption of zero cavitation is reasonable as long as $|p_+-p_\infty|\ll|p_--p_\infty|$. It is noted that the upwash is considered unknown on blade surfaces exposed to the separated flow. Also, it is assumed that flow separation occurs only on the suction side of the airfoil.

In summary, we will seek the solution of Eq. (3) subject to the boundary conditions [Eqs. (6) and (7)], as well as the con-

dition of pressure and normal velocity continuity in the wake and the radiation/finiteness condition. Note that Eq. (6) applies to the lower pressure surface ($z=0^-$) and the portion of the upper suction surface ($z=0^+$) where the mean flow is attached, while the upwash is considered unknown on the portion of the surface where flow separation occurs.

Solution Procedures

The Fourier transform pair is defined as

$$\phi^* = \int_{-\infty}^{\infty} \phi e^{-i\alpha x} dx$$
$$\phi = \frac{1}{2\pi}\int_{-\infty}^{\infty} \phi^* e^{i\alpha x} d\alpha \tag{8}$$

Applying Fourier transform to Eqs. (3), (4), and (6), one obtains

$$\frac{d^2\phi^*}{dz^2} + \mu^2\phi^* = 0 \tag{9}$$

where

$$\mu^2 = \beta^2\left[\left(\frac{\omega}{U}\frac{M}{\beta^2}\right)^2 - \left(\alpha - \frac{\omega}{U}\frac{M^2}{\beta^2}\right)^2\right]$$

and

$$\frac{p^*}{\rho U} = -i\left(\frac{\omega}{U}+\alpha\right)\phi^* \tag{10}$$

subject to the boundary conditions,

$$\phi_z^* = W_+^* \quad \text{at} \quad z=0^+ \tag{11}$$

$$\phi_z^* = W_-^* \quad \text{at} \quad z=0^- \tag{12}$$

where W_+^* and W_-^* are the Fourier transforms of the upwashes on the upper and lower surfaces of the airfoil, respectively. As shown in Ref. 17, the transformed perturbation pressures on the airfoil surfaces are

$$\frac{p_+^*}{\rho U^2} = -\frac{\omega/U+\alpha}{\mu}\frac{W_+^*}{U} \tag{13}$$

$$\frac{p_-^*}{\rho U^2} = \frac{\omega/U+\alpha}{\mu}\frac{W_-^*}{U} \tag{14}$$

where

$$\mu = \begin{cases} i|\mu| & \text{for} \quad \alpha>\alpha_1 \text{ or } \alpha>\alpha_2 \\ -|\mu| & \text{for} \quad \alpha_1<\alpha<\alpha_2 \end{cases}$$

$$|\mu| = \beta\left|\left(\omega/U\frac{M}{\beta^2}\right)^2 - \left(\alpha-\omega/U\frac{M^2}{\beta^2}\right)^2\right|^{1/2} \geq 0$$

$$\alpha_1 = -\omega/(a+U)$$

$$\alpha_2 = \omega/(a-U)$$

Since we are interested in pressure differences, define Δp^* and $\bar{p}^*$ as

$$\Delta p^* = p_+^* - p_-^* \quad \bar{p}^* = \tfrac{1}{2}(p_+^* + p_-^*) \tag{15}$$

Similarly, define ΔW^* and $\bar{W}^*$ as

$$\Delta W^* = W_+^* - W_-^* \quad \bar{W}^* = \tfrac{1}{2}(W_+^* + W_-^*) \tag{16}$$

Using Eqs. (15) and (16) in Eqs. (13) and (14), we obtain

$$\bar{W}^*/U = K^*(\Delta p^*/\rho U^2) \tag{17}$$

$$\bar{p}^*/\rho U^2 = A^*(\Delta W^*/U) \tag{18}$$

where

$$K^* = -\frac{1}{2}\frac{\mu}{(\omega/U)+\alpha} \tag{19}$$

$$A^* = -\frac{1}{2}\frac{(\omega/U)+\alpha}{\mu} \tag{20}$$

A Fourier inversion of Eq. (17) yields

$$\frac{\bar{W}(x)}{U} = \int_0^1 K(x-\xi)\frac{\Delta p(\xi)}{\rho U^2}d\xi \tag{21}$$

where the lifting kernel K is the Fourier inversion of K^*. For attached flows, $\bar{W}(x)$ is known in terms of the airfoil vibration mode shape and Eq. (21) can be solved easily. The domain of integration of the integral in Eq. (21) covers only the airfoil surface because we consider thin wakes and assume continuous pressure across the wake itself. For separated flows, $\bar{W}(x)$ is unknown for separated region on the airfoil ($x_s<x<1$), although it is prescribed for the rest of the airfoil ($0<x<x_s$). Hence, the left-hand side of Eq. (21) is partially unknown. Apparently, an additional equation is needed in order to solve for the unknown upwash velocity in separated region on the airfoil. In fact, if ΔW is known, $\bar{W}$ can be calculated by

$$\bar{W} = \tfrac{1}{2}(W_+ + W_-) = W_- + \tfrac{1}{2}\Delta W \tag{22}$$

since W_- is known completely from Eq. (6).

To derive an integral equation for ΔW, we formally invert Eq. (21) to obtain

$$\frac{\Delta p(x)}{\rho U^2} = \int_0^1 \Gamma_K(x,\xi)\frac{\bar{W}(\xi)}{U}d\xi \tag{23}$$

where Γ_K is the resolvent kernel corresponding to the lifting kernel function K. General procedures are available to calculate Γ_K for a given K with fairly general singular behavior.[18,19]

A Fourier inversion of Eq. (18) yields

$$\frac{\bar{p}(x)}{\rho U^2} = \int_{x_s}^1 A(x-\xi)\frac{\Delta W(\xi)}{U}d\xi \tag{24}$$

where we have used the condition that the upwash difference ΔW is zero both off the airfoil ($x<0, x>1$) and over the attached flow portion of the airfoil ($0<x<x_s$).

In separated region $\hat{p}+ = -\tfrac{1}{2}\rho U^2\gamma$ from Eq. (7), i.e.,

$$\bar{p} + \Delta p/2 = -\tfrac{1}{2}\rho U^2\gamma \tag{25}$$

Substitution of Eqs. (23) and (24) into Eq. (25) yields

$$\int_{x_s}^1 A(x-\xi)\frac{\Delta W(\xi)}{U}d\xi + \tfrac{1}{2}\int_0^1 \Gamma_K(x,\xi)\frac{\bar{W}(\xi)}{U}d\xi = -\frac{\gamma}{2} \tag{26}$$

Now, from Eq. (22),

$$\bar{W} = W_- + \tfrac{1}{2}\Delta W$$

Hence, Eq. (26) becomes

$$\int_{x_s}^1 C(x,\xi)\frac{\Delta W(\xi)}{U}d\xi = \ell(x) - \frac{\gamma}{2} \tag{27}$$

where

$$\ell(x) = -\tfrac{1}{2}\int_0^1 \Gamma_K(x,\xi)\frac{W_-(\xi)}{U}d\xi \tag{28}$$

$$C(x,\xi) = A(x-\xi) + \tfrac{1}{4}\Gamma_K(x,\xi) \tag{29}$$

Note that ΔW has been set to zero over the attached flow portion of the airfoil ($0<x<x_s$) as assumed earlier. It is seen from Eq. (28) that the function $\ell(x)$ is actually proportional to the pressure differential for attached (i.e., nonseparated) flows, i.e.,

$$\ell(x) = -\tfrac{1}{2}\frac{\Delta_{P_{NS}}(x)}{\rho U^2} \tag{30}$$

III. Formulas

This section presents the mathematical expressions and formulas required for airload calculations. Only the key results are given here; for more details, see Ref. 17.

Kernel Functions

The kernel functions K and A need to be calculated by the Fourier inversions of K^* and A^* given in Eqs. (19) and (20). Physically, K is the upwash due to an impulse pressure differential and A the perturbation pressure due to an impulse averaged upwash. Usually, K is called the lifting kernel and A the nonlifting kernel. Analytical inversion results are given by the following formulas.

The lifting kernel $K(x)$ is simply the well-known Possio's kernel containing a singular part K_s and a regular part K_c,

$$K(x) = K_s(x) + K_c(x)$$

where

$$K_s(x) = \frac{\beta}{2\pi x} - \frac{i}{2\pi\beta}\frac{\omega}{U}\ell n\left|\frac{\omega x}{U}\right|$$

$$K_c(x) = -\frac{\omega}{U}\frac{1}{4\beta}\left\{\left[e^{i(M^2/\beta^2)(\omega x/U)}iM\,\mathrm{sgn}(x)\right.\right.$$

$$\times H_1^{(2)}\left(\frac{M}{\beta^2}\left|\frac{\omega x}{U}\right|\right) + \frac{2\beta^2}{\pi}\frac{U}{\beta x}\Bigg]$$

$$-\left[e^{i(M^2/\beta^2)(\omega x/U)}H_0^{(2)}\left(\frac{M}{\beta^2}\left|\frac{\omega x}{U}\right|\right) + i\frac{2}{\pi}\ell n\left|\frac{\omega x}{U}\right|\right]$$

$$+ i\beta^2 e^{-i(\omega x/U)}\left[\frac{2}{\pi\beta}\ell n\frac{1+\beta}{M}\right.$$

$$\left.\left.+\int_0^{(1/\beta^2)(\omega x/U)} e^{-iu}H_0^{(2)}(M|u|)\,\mathrm{d}u\right]\right\}$$

The nonlifting kernel $A(x)$ also contains a singular part and a regular part,

$$A(x) = A_s(x) + A_c(x)$$

where

$$A_s(x) = \frac{-1}{2\pi\beta x} - \frac{i}{2\pi\beta^3}\frac{\omega}{U}\ell n\left|\frac{\omega x}{U}\right|$$

$$A_c(x) = \frac{1}{4\beta^3}\frac{\omega}{U}\left\{\left[e^{i(M^2/\beta^2)(\omega x/U)}H_0^{(2)}\left(\frac{M}{\beta^2}\left|\frac{\omega x}{U}\right|\right)\right.\right.$$

$$\left.+ i\frac{2}{\pi}\ell n\left|\frac{\omega x}{U}\right|\right] + \left[e^{i(M^2/\beta^2)(\omega x/U)}iM\,\mathrm{sgn}(x)\right.$$

$$\left.\left.+H_1^{(2)}\left(\frac{M}{\beta^2}\left|\frac{\omega x}{U}\right|\right) + \frac{2}{\pi}\beta^2\frac{U}{\omega x}\right]\right\}$$

Inversion Kernel $\Gamma_K(x,\xi)$

If any two basic solutions of Eq. (21), such as the unit upwash solution and the homogeneous solution of Eq. (21) denoted by $P_1(x)$ and $P_0(x)$, respectively, are known, the inversion kernel can be written as[18,19]

$$\Gamma_K(x,\xi) = P_0(1-\xi)P_1(x) - \frac{\partial G(x,\xi)}{\partial\xi}$$

where

$$\frac{\partial G}{\partial\xi}(x,\xi) = [A_1 + 2A_2(\xi-x)]G_{01}(x,\xi)$$

$$+ [A_0 + A_1(\xi-x) + A_2(\xi-x)^2]\frac{\partial G_{01}}{\partial\xi}(x,\xi)$$

$$+ B_1Q_1(x)Q_1(\xi) \quad + [B_0 + B_1(\xi-x)]Q_1(x)\frac{\partial Q_1(\xi)}{\partial\xi}$$

$$- C_0Q_2(x)\frac{\partial Q_2(\xi)}{\partial\xi}$$

$$G_{01}(x,\xi) = 2\ell n\left|\frac{\sqrt{(1-\xi)/\xi} + \sqrt{(1-x)/x}}{\sqrt{(1-\xi)/\xi} - \sqrt{(1-x)/x}}\right|$$

$$\frac{\partial G_{01}}{\partial\xi}(x,\xi) = \frac{2}{x-\xi}\cdot\frac{x(1-x)}{\xi(1-\xi)}$$

$$Q_1(x) = 2\sqrt{x(1-x)}$$

$$Q_2(x) = 4(2x-1)\sqrt{x(1-x)}$$

$$\frac{\partial Q_1(\xi)}{\partial\xi} = \frac{1-2\xi}{\sqrt{\xi(1-\xi)}}$$

$$\frac{\partial Q_2(\xi)}{\partial\xi} = 4Q_1(\xi) - 2(1-2\xi)\frac{\partial Q_1(\xi)}{\partial\xi}$$

$$A_0 = d_{01} + d_{03} + d_{23} - d_{12}$$

$$A_1 = 4(2d_{13} - d_{02})$$

$$A_2 = 16d_{03}$$

$$B_0 = 4d_{12} - 4d_{23} - 8d_{03}$$

$$B_1 = -16d_{13}$$

$$C_0 = 2d_{23}$$

$$d_{ij} = (\hat{b}_i b_j - b_i\hat{b}_j)/[\pi(b_0\hat{b}_0)]$$

$$b_0 = \frac{\alpha_0}{2} + \frac{\alpha_1}{8} + \frac{\alpha_2}{16} \qquad \hat{b}_0 = \frac{\hat{\alpha}_0}{2} + \frac{3}{8}\hat{\alpha}_1 + \frac{5}{16}\hat{\alpha}_2$$

$$b_1 = -\frac{\alpha_0}{2} + \frac{\alpha_2}{32} \qquad \hat{b}_1 = \frac{\hat{\alpha}_0}{2} + \frac{\hat{\alpha}_1}{2} + \frac{15}{32}\hat{\alpha}_2$$

$$b_2 = -\frac{\alpha_1}{8} - \frac{\alpha_2}{16} \qquad \hat{b}_2 = \frac{\hat{\alpha}_1}{8} + \frac{3}{16}\hat{\alpha}_2$$

$$b_3 = -\frac{\alpha_2}{32} \qquad \hat{b}_3 = \frac{\hat{\alpha}_2}{32}$$

$$\alpha_n = 2a_n \qquad \hat{\alpha}_n = -2\hat{a}_n$$

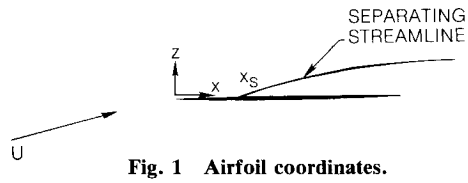

Fig. 1 Airfoil coordinates.

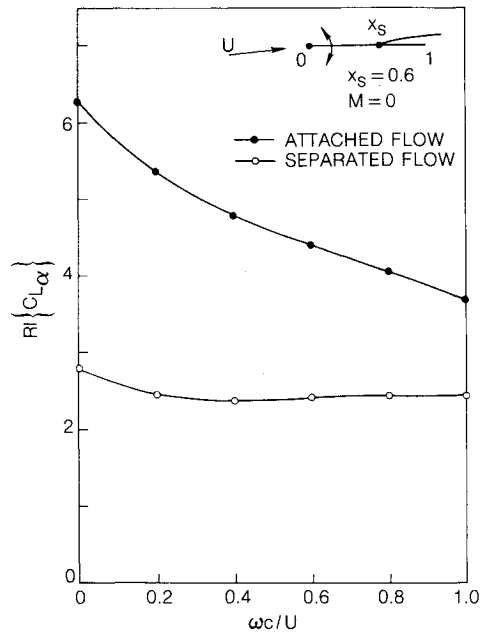

Fig. 2 Real part of lift coefficient due to pitching motion about leading edge.

Here a_n and $\hat{a}_n$ are defined as the expansion coefficients of the unit upwash solutions $P_1(x)$ and $\hat{P}_1(x)$,

$$P_1(x) = 2\sqrt{1-x/x}\sum_{n=0}^{N-1} a_n x^n$$

$$\hat{P}_1(x) = -2\sqrt{1-x/x}\sum_{n=0}^{N-1} \hat{a}_n x^n$$

where N is the number of pressure modes. The constant coefficients a_n and $\hat{a}_n$ are chosen so that $P_1(x)$ and $\hat{P}_1(x)$ satisfy the following unit upwash integral equations at N collocation points and also the leading and trailing edge Kutta conditions, respectively:

$$\int_0^1 K(x-\xi)P_1(\xi)\mathrm{d}\xi = 1 \quad P_1(1) = 0$$

$$\int_0^1 K(x-\xi)\hat{P}_1(\xi)\mathrm{d}\xi = 1 \quad \hat{P}_1(0) = 0$$

Finally, the homogeneous solution or eigensolution $P_0(x)$ is defined as

$$P_0(x) = \frac{P_1(x) - \hat{P}_1(x)}{\pi(b_0 - \hat{b}_0)}$$

so that

$$\int_0^1 P_0(x)\mathrm{d}x = 1$$

Solution for Wake Upwash Difference $\Delta W(x)$

The solution for the wake upwash difference depends on the trailing-edge upwash condition imposed. Here, we discuss the solution procedures that produce the best correlation with test

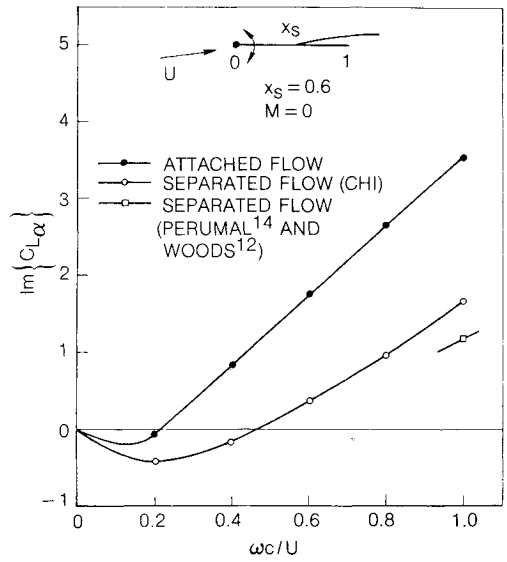

Fig. 3 Imaginary part of lift coefficient due to pitching motion about leading edge.

data. More discussion on this issue is given in Sec. IV. In Eq. (27), the new kernel function $C(x,\xi)$ has a predominant Cauchy type of singularity at $\xi = x$ and has a square-root type of singularity at $\xi = 1$. To render the integral equation (27) to a purely Cauchy-type integral equation, we write

$$\int_{x_s}^1 \sqrt{1-\xi}C(x,\xi)\frac{\Delta W(\xi)}{U\sqrt{1-\xi}}\mathrm{d}\xi = \ell(x) - \frac{\gamma}{2}$$

Furthermore, from Eq. (30) $\ell(x) \sim 1/\sqrt{x}$ as $x \to 0$. To arrive at a regular forcing function, we write

$$\int_{x_s}^1 \left[\sqrt{x(1-\xi)}C(x,\xi)\right]\frac{\Delta W(\xi)}{U\sqrt{1-\xi}}\mathrm{d}\xi = \sqrt{x}\left(\ell(x) - \frac{\gamma}{2}\right) \tag{31}$$

This purely Cauchy-type integral equation has the following solution:

$$\frac{\Delta W(\xi)}{U\sqrt{1-\xi}} = \sqrt{1-\xi^*}\sum_{n=1}^{N} a_n^W \xi^{*n-3/2} \tag{32}$$

where

$$\xi^* \equiv (\xi - x_s)/(1-x_s)$$

Here, we have imposed the condition $\Delta W(1) = 0$ consistent with the boundary condition $\Delta W(x) = 0$, for $x > 1$, for a smooth trailing-edge flow. Therefore,

$$\frac{\Delta W(\xi)}{U} = \frac{1-\xi}{\sqrt{1-x_s}}\sum_{n=1}^{N} a_n^W \xi^{*n-3/2} \tag{33}$$

Substitution of Eq. (32) into the left-hand side of Eq. (31) gives

$$\sum_{n=1}^{N} a_n^W E_n(x) = \sqrt{x}\left[\ell(x) - \frac{\gamma}{2}\right] \tag{34}$$

where

$$E_n(x) = \int_{x_s}^1 \sqrt{x(1-\xi)}C(x,\xi)\sqrt{1-\xi^*}\xi^{*n-3/2}\mathrm{d}\xi$$

Given $\ell(x)$ from Eq. (30), one can solve Eq. (34) by the collocation method to obtain a_n^w. Then Eq. (33) gives the desired $\Delta W(x)$.

Lift and Moment Formulas

The pressure differential solution of Eq. (23) can be written as

$$\Delta p(x) = \Delta p_{\mathrm{NS}}(x) + \Delta p_{\mathrm{COR}}(x)$$

where

$\Delta p_{\mathrm{NS}}(x)$ = pressure differential as if no flow separation occurs

$$= \rho U^2 \int_0^1 \Gamma_K(x,\xi) \frac{\bar{W}_{\mathrm{NS}}}{U}(\xi)\,\mathrm{d}\xi$$

$\Delta p_{\mathrm{COR}}(x)$ = additional pressure differential contribution due to flow separation or flow separation correction pressure

$$= \rho U^2 \int_{x_s}^1 \frac{1}{2} \Gamma_K(x,\xi) \frac{\Delta W(\xi)}{U}\,\mathrm{d}\xi$$

Consequently, the lift and moment (about $x = x_0$) coefficients are both sums of a nonseparated flow part and a separation correction part,

$$C_L = -\int_0^1 \Delta p(x)\,\mathrm{d}x \Big/ \tfrac{1}{2}\rho U^2 c = C_{L_{\mathrm{NS}}} + C_{L_{\mathrm{COR}}}$$

$$C_M = \int_0^1 (x - x_0)\Delta p(x)\,\mathrm{d}x \Big/ \tfrac{1}{2}\rho U^2 c^2 = C_{M_{\mathrm{NS}}} + C_{M_{\mathrm{COR}}}$$

where

$$C_{L_{\mathrm{NS}}} = -4 \sum_{j=1}^{N} a_j f_j$$

$$C_{M_{\mathrm{NS}}} = x_0 C_{L_{\mathrm{NS}}} - 4 \sum_{j=1}^{N} a_j f_{j+1}$$

$$C_{L_{\mathrm{COR}}} = -2 \sum_{i=1}^{N} a_i^W \sum_{j=1}^{N} e_j (1 - x_s)^j I_{ij}$$

$$C_{M_{\mathrm{COR}}} = x_0 C_{L_{\mathrm{COR}}} + 2 \sum_{i=1}^{N} a_i^w \sum_{j=1}^{N} (e_j - r_j)(1 - x_s)^j I_{ij}$$

$$I_{ij} = \int_0^1 Z^{j-3/2} (1 - Z)^{j-1/2} [x_s + (1 - x_s)Z]^{1/2}\,\mathrm{d}Z$$

$$f_j = \frac{\sqrt{\pi}}{2} \frac{\Gamma(j - \tfrac{1}{2})}{\Gamma(j+1)}$$

$$f_{j+1} = \frac{j - \tfrac{1}{2}}{j+1} f_j$$

For leading-edge separation ($x_s = 0$), we have the following simpler formulas:

$$C_{L_{\mathrm{COR}}} = -2 \sum_{i=1}^{N} a_i^w \sum_{j=1}^{N} e_j B_{ij}$$

$$C_{M_{\mathrm{COR}}} = x_0 C_{L_{\mathrm{COR}}} + 2 \sum_{i=1}^{N} a_i^W \sum_{j=1}^{N} (e_j - r_j) B_{ij}$$

where the beta function is defined as

$$B_{ij} = \frac{\Gamma(i)\Gamma(j + \tfrac{1}{2})}{\Gamma(i + j + \tfrac{1}{2})}$$

The coefficients a_j are the coefficients of the nonseparated flow pressure expansion,

$$\frac{\Delta p(x)}{\rho U^2} = 2\sqrt{1 - x/x} \sum_{j=1}^{N} a_j x^{j-1}$$

as a solution of Eq. (21). The coefficients a_j^w are the upwash coefficients in Eq. (33). The coefficients e_j and r_j are coefficients of the expansions of two elementary solutions $P_1(x)$ and $P_2(x)$ that satisfy the trailing-edge Kutta condition and the following singular integral equations:

$$\int_0^1 K(x - \xi) P_1(\xi)\,\mathrm{d}\xi = 1 \quad P_1(1) = 0$$

$$\int_0^1 K(x - \xi) P_2(\xi)\,\mathrm{d}\xi = x \quad P_2(1) = 0$$

$$P_1(x) = 2\sqrt{1 - x/x} \sum_{n=1}^{N} e_n x^{n-1}$$

$$P_2(x) = 2\sqrt{1 - x/x} \sum_{n=1}^{N} r_n x^{n-1}$$

IV. Remarks on Wake Upwash Difference Solution $\Delta W(x)$

The solution for the wake upwash difference $\Delta W(x)$ from the singular integral equation (27) is not unique unless one specifies enough constraints to the behavior of the upwash difference $\Delta W(x)$ a priori. A physically meaningful way to specify the constraints is to compare the experimental lift and/or moment coefficients with the theoretical prediction results while assuming various types of constraints. This strategy of specifying constraints was used in Ref. 16 in studying stalled airloads for cascade blades. The same constraints on the wake upwash difference $\Delta W(x)$ are used in this paper for isolated airfoils. These constraints require that the wake upwash difference $\Delta W(x)$ vanish at the airfoil trailing edge and be differentiable at the airfoil trailing edge. See Eq. (32) for these constraints.

Another possible choice of constraints is to still impose the constraint of zero wake upwash difference at the trailing edge, $\Delta W(1) = 0$, but to assume a square root type of wake upwash difference near the trailing edge, $\Delta W(x) \sim \sqrt{1 - x}$. This choice of constraints does not yield good correlations between calculated and experimental data on force coefficients, but it does result in force coefficients close to the theoretical results of Woods[12] and Perumal and Sisto.[14] It should be noted that both Woods and Perumal and Sisto assume a zero unsteady pressure, not only over the airfoil surface where separation region exists, but also within the wake region extending to downstream infinity. On the other hand, the separated flow theory presented in this paper assumes a constant unsteady pressure (chosen as zero in all calculations, however) over the airfoil surface where the flow separation exists (just as Woods[12] and Perumal and Sisto[14] do), but specifies a pressure continuity condition $\Delta p = 0$ across the wake boundary instead.

Based on the above discussion and the calculated results to be discussed in Sec. V, it appears that the assumption of zero pressure in the wake region behind the trailing edge is not physically justifiable. The present theory assuming a differentiable wake upwash difference and a pressure continuity behind the trailing edge, however, yields good correlation with test data and therefore appears more appropriate. The closeness between 1) the solution by assuming a zero pressure in the wake region behind the trailing edge and 2) the solution based on present theory assuming a square-root type of wake upwash difference near the trailing edge is simply fortuitous.

V. Results

The discussion of the calculated results are divided into two parts. In the first part, comparisons are made between the

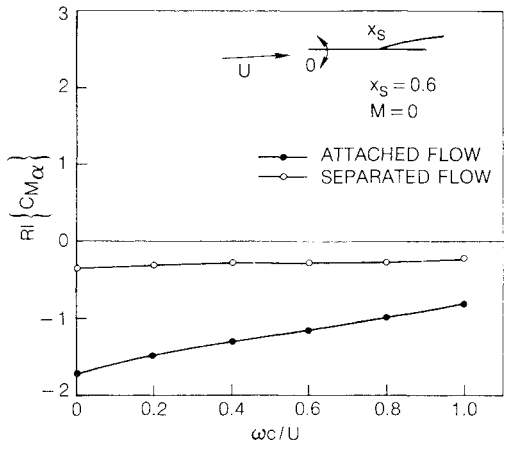

Fig. 4 Real part of moment coefficient due to pitching motion about leading edge.

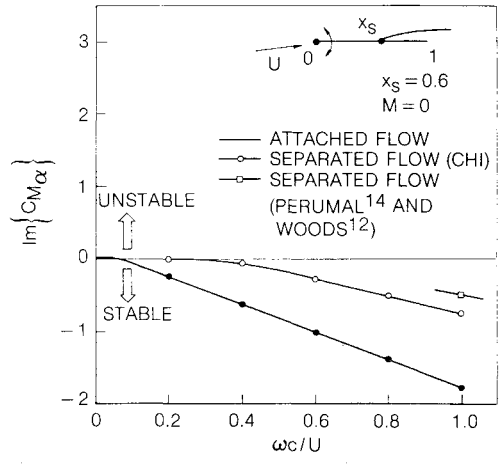

Fig. 5 Imaginary part of moment coefficient due to pitching motion about leading edge.

results based on the present theory and other theories. In the second part, experimental data are used to validate the present theory.

Comparison with Other Theories—Square-Root Type of Upwash

For a thin airfoil in a zero Mach number flow that separates at 60% chord on the upper surface, Figs. 2-5 show the real and imaginary parts of the calculated lift and moment coefficients for a pitching oscillation about the leading edge in the reduced frequency range of 0-1.0. Also shown in these figures are the corresponding force coefficients predicted by attached flow flat-plate theory. Flow separation is seen to reduce the magnitudes of the airloads over the entire frequency range and tends to destabilize the pitching motion as seen in Fig. 5. The predicted imaginary parts of the lift and moment coefficients agree well with those of Perumal[14] and Woods.[12] This agreement, however, does not imply that a physically meaningful prediction has been made as was discussed in Sec. IV. A successful prediction should be based on good correlations with test data from carefully performed experiments.

Comparison with Experimental Damping—Differentiable Upwash

Lemnios[20] performed excellent aeroelastic tests of NACA 16-series airfoil sections for Hamilton Standard 18A20 propeller blade and Curtiss-Wright 109640 propeller blade. The blade sections are as shown in Fig. 6. The aerodynamic damping (i.e., negative of the moment coefficient for pitching motion) data for the thinnest section 16 (070)(023) of the Hamilton Standard 18A20 propeller blade are used to evaluate

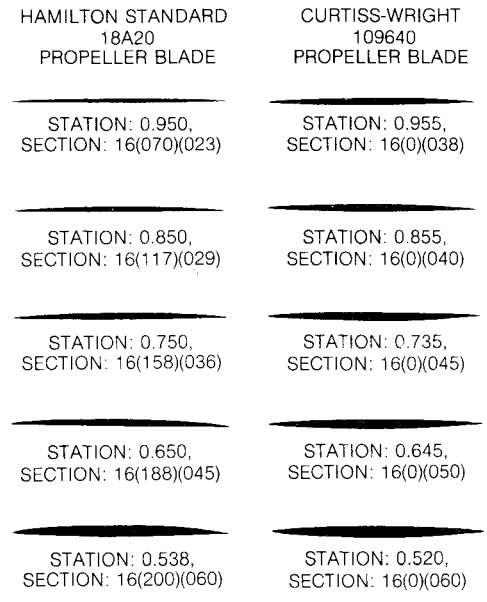

Fig. 6 Profiles of NACA 16-series airfoils.

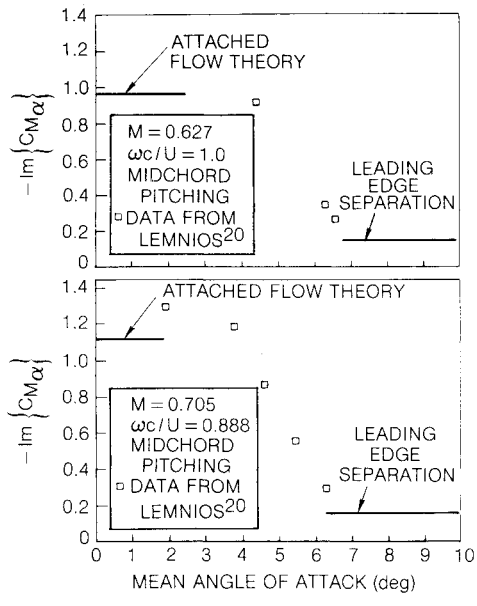

Fig. 7 Torsional aerodynamic damping for section 16(070)(023) of HS 18A20 propeller.

the present theory. In Figs. 7 and 8, the measured aerodynamic dampings for a small-amplitude pitching oscillation about the midchord at various mean angles of attack are compared to the classical attached and separated flow results (assuming leading-edge flow separations) for four sets of Mach number/reduced-frequency combinations.

The leading-edge separation results appear to represent the asymptotic damping at large angles of attack in all cases. The correlation between theory and experiment here is very encouraging. The test data for intermediate angles of attack can probably be correlated with the separated flow unsteady aerodynamic theory by varying the flow separations point along the airfoil chord. This idea has not been explored further because of the lack of clear criteria to determine the flow separation point. However, by comparing theoretical calculations for various flow separation points with test data, promising flow separation criteria can probably be generated for flutter prediction purposes.

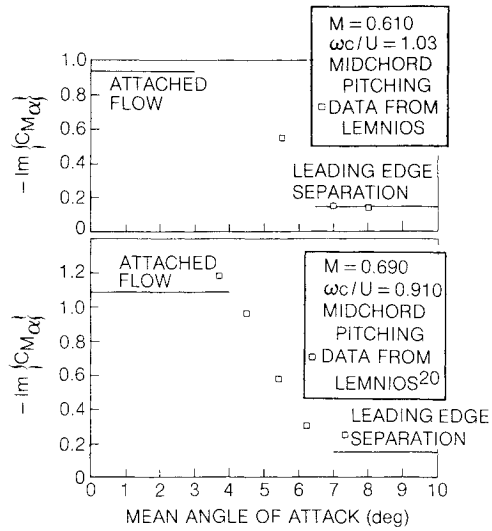

Fig. 8 Torsional aerodynamic damping for section 16(070)(023) HS 18A20 propeller.

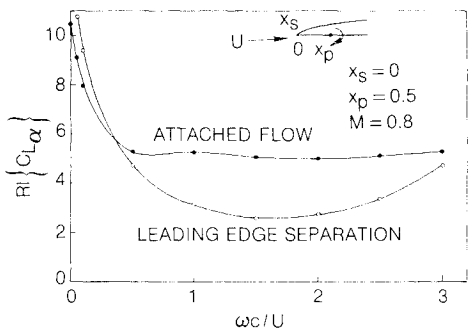

Fig. 9 Real part of lift coefficient due to pitching motion about midchord.

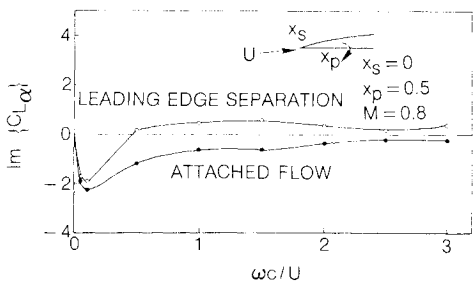

Fig. 10 Imaginary part of lift coefficient due to pitching motion about midchord.

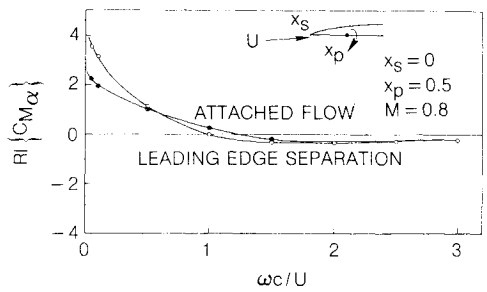

Fig. 11 Real part of moment coefficient due to pitching motion about midchord.

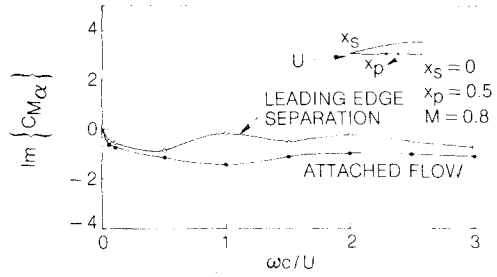

Fig. 12 Imaginary part of moment coefficient due to pitching motion about midchord.

To illustrate the force coefficients for a given Mach number over a wide frequency range, the lift and moment coefficients for a midchord pitching airfoil in a subsonic flow with Mach number 0.8 are shown in Figs. 9-12, for both the attached flow and the leading-edge separated flow. The pitch damping is seen to decrease as separation is introduced in Fig. 12. Meanwhile, a positive imaginary part of the lift coefficient due to pitching motion is predicted for separated flow as shown in Fig. 10. This implies that the bending component in a blade mode shape could be driven into instability by the destabilizing lift force due to the torsional component of the blade mode shape if leading-edge flow separation occurs.

VI. Conclusions and Recommendations

A relatively simple two-dimensional linear unsteady aerodynamic theory has been developed to take into account the effect of flow separation on unsteady airloads for thin airfoils oscillating in a subsonic airstream. The theory is essentially a modification of the classical potential flow unsteady aerodynamic theory. The modification involves the specification of a constant (taken as zero in this paper) pressure in the flow separation zone along the blade surface. As a result, the upwash velocity in the flow separation zone is solved as part of the problem solution. Proper constraints on the upwash velocity in the separation zone are imposed based on the correlation between calculated and experimental aerodynamic damping data for thin airfoil sections. Two different types of upwash velocity constraints were studied. One type of constraint requires a square-root type of behavior near the airfoil trailing edge and is shown to resemble closely the earlier theories of Woods, Perumal, and Sisto, which assume a zero pressure on the separated airfoil surface as well as in the wake region behind the airfoil trailing edge. This type of constraint, however, does not yield results consistent with the available test data. The other type of constraint requires the differentiability of the wake upwash velocity near the trailing edge and yields theoretically calculated torsional damping values in good agreement with test data of Lemnios for thin airfoils used in typical propeller designs.

The assumption of zero pressure in the separated flow region is perhaps reasonable at low frequencies. For high frequencies, other assumptions such as piston theory could be made. For intermediate frequencies, logical composite pressure expressions using zero pressure and piston theory asymptotes can probably be developed and used as the theoretical basis for further correlation of the separated flow theory with test data of thin airfoils at various angles of attack.

The present theory assumes that the flow separation point is known either from theory or experiment. A separate theory to predict the flow separation point must be based on steady viscous flow models involving boundary-layer considerations. On the other hand, experimental verification of flow separations would involve flow visualizations. Both approaches require substantial amounts of effort, but the experimental approach appears most direct in producing the

flow separation information as input to the present unsteady aerodynamic theory for separated flows.

For supercritical flows, the existence of shock waves is a distinct feature of the flowfield and the shock movement associated with the blade motion may be the major contributing mechanism to the unsteady airload. Furthermore, for high-angle-of-attack flows, the effects of shock waves and flow separations on unsteady airloads are likely to be equally important. An extension of the present separated flow theory to include shock waves appears possible and potentially significant for airfoil flutter design applications to supercritical flight conditions.

Acknowledgments

This work was sponsored by the Hamilton Standard Division and the United Technologies Research Center of the United Technologies Corporation. The basic idea of the flow model and solution approach originated from a paper by Earl H. Dowell.[15] The discussion with Marc H. Williams constituted an important part of this work, especially in developing the analytical form of the inversion kernel.

References

[1]Williams, L. J., "Small Transport Aircraft Technology," NASA SP-460, 1983.

[2]Lubomski, J. K., "SR5-10 Way Strain Gage Data," Personal notes, 1982.

[3]Smith, A. M. O., "Remarks on Fluid Mechanics of the Stall," *Aircraft Stalling and Buffeting*, AGARD-LS-74.

[4]Ericsson, L. E. and Reding, J. P., "Unsteady Airfoil Stall, Review and Extension," *AIAA Journal*, Vol. 8, Aug. 1981, pp. 609-616.

[5]Ericsson, L. E. and Reding, J. P., "Analytic Prediction of Dynamic Stall Characteristics," AIAA Paper 72-682, June 1972.

[6]Ericsson, L. E., "Dynamic Effects of Shock-Induced Flow Separation," *Journal of Aircraft*, Vol. 12, Feb. 1975, pp. 86-92.

[7]Ericsson, L. E. and Reding, J. P., "Effect of Angle of Attack and Mach Number on Slender Wing Aerodynamics," AIAA Paper 77-667, June 1977.

[8]Ham, N. D., "Aerodynamic Loading on a Two Dimensional Airfoil during Dynamic Stall," *AIAA Journal*, Vol. 6, Oct. 1968, pp. 1927-1934.

[9]Kandil, O. A., Chu, L. C., and Yates, E. C., Jr., "Hybrid Vortex Method for Lifting Surfaces with Free Vortex Flow," AIAA Paper 80-0070, Jan. 1980.

[10]Kandil, O. A., Chu, L. C., and Tureaud, T., "Steady and Unsteady Nonlinear Hybrid Vortex Method for Lifting Surfaces at Large Angle of Attack," AIAA Paper 82-0351, Jan. 1982.

[11]Kandil, O. A., "A Technique for Three-Dimensional Compressible Flow Past Wings at High Angles of Attack," AIAA Paper 83-2078, Aug. 1981.

[12]Woods, L. C., "Aerodynamic Forces on an Oscillating Aerofoil Fitted With a Spoiler," *Proceedings of the Royal Society of London*, Ser. A, No. 239, 1957, pp. 328-337.

[13]Wu, T. Yao-Tsu, "A Wake Model for Free-Streamline Flow Theory, Part 1: Fully and Partially Developed Wake Flows and Cavity Flows Past an Oblique Flat Plate," *Journal of Fluid Mechanics*, Vol. 13, 1962, pp. 161-181.

[14]Perumal, P. V. K. and Sisto, F., "Lift and Moment Prediction for an Oscillating Airfoil with a Moving Separation Point," *ASME Transactions, Journal of Engineering for Power*, Vol. 96, Oct. 1974, pp. 372-378.

[15]Dowell, E. H., "A Simplified Theory of Oscillating Airfoils in Transonic Flow: Review and Extension," AIAA Paper 77-445, March 1977.

[16]Chi, R. M., "Unsteady Aerodynamics in Stalled Cascade and Stall Flutter Prediction," ASME Paper 80-C2/Aero-1, 1980.

[17]Chi, R. M., "Separated Flow Unsteady Aerodynamics for Propfan Applications," United Technologies Research Center, East Hartford, CT, Rept. R83-356891-1, July 1983.

[18]Williams, M. H., "The Inversion of Singular Integral Equations by Expansion in Jacobi Polynominals," Paper presented at 8th U.S. Congress of Applied Mechanics, Los Angeles, June 1978.

[19]Williams, M. H., "The Resolvent of Singular Integral Equations," *Quarterly of Applied Mathematics*, Vol. 35, No. 1, April 1977, pp. 99-110.

[20]Lemnios, A. Z., "Aerodynamic Damping Tests of Propeller Blade Airfoil Sections," United Aircraft Research Laboratory, East Hartford, CT, Rept. R-0997-1, Oct. 1957.